# Partial discretization solution for flexure of a circular plate

**Batyrkhan Kyrykbayev**[1]**, Auezkhan Turdaliev**[2]**, Roza Koilybayeva**[3]**, Algazy Zhauyt**[4]
[1, 2]International University of Transportation and Humanities, Almaty, 050036, Kazakhstan
[3, 4]Department of Aerospace and Electronic Engineering, Almaty University of Power Engineering and Telecommunications named after G. Daukeyev, Almaty, 050013, Kazakhstan
[1]Corresponding author
**E-mail:** [1]*kyrykbaev.batyrkhan@mail.ru*, [2]*auezkhan_tur@mail.ru*, [3]*r.koilybaeva@aues.kz*, [4]*a.zhauyt@aues.kz*

*Received 23 April 2026; accepted 22 June 2026; published online 16 July 2026*
*DOI https://doi.org/10.21595/vp.2026.26589*

Check for updates

*77th International Conference on Vibroengineering in Almaty, Kazakhstan, June 11-12, 2026*



**Abstract.** This paper presents an analytical solution for the axisymmetric flexure problem of a rotationally symmetric circular plate using the method of partial discretization of differential equations. The plate is considered under transverse loading and radial boundary action, which lead to a fourth-order differential equation describing the deflection of the plate. Since direct analytical integration of the governing equation may be difficult for non-uniform loading and boundary conditions, the partial discretization approach is applied to transform the original problem into a more convenient analytical-discrete form. Explicit expressions are obtained for the plate deflection, rotation angle, bending moments, and transverse shear force. The derived solution makes it possible to evaluate the influence of radial boundary load on the deformation behavior of the circular plate. Numerical examples and graphical results demonstrate that increasing the radial load leads to a systematic increase in deflection and internal force factors. The obtained results confirm the effectiveness of the proposed method and show its applicability for engineering analysis of circular plates and thin-walled structural elements subjected to axisymmetric loading.

**Keywords:** annular plate, nonlinear bending, stress function, plate deflection, radial stress.

## 1. Introduction

Recent investigations of nonlinear bending in thin plates and cylindrical shells have employed a wide range of analytical and numerical approaches [1]. Analytical and semi-analytical methods remain valuable because they reveal the direct influence of geometric parameters, load intensity, boundary conditions, and thermal gradients on the structural response. Perturbation methods, variational formulations [2], differential transformation techniques, and integral-based procedures have been used to derive approximate solutions for plates and shells subjected to nonlinear mechanical and thermal actions. At the same time, finite element, finite difference, mesh-free, and spectral methods provide flexible tools for investigating complex geometries, variable material properties, large deflections, and combined loading conditions [3]. However, for shells with variable thickness and spatially non-uniform temperature fields, numerical calculations may obscure the explicit relationship between design parameters and deformation characteristics. Therefore, the development of analytical-discrete methods remains important for obtaining interpretable engineering solutions while retaining the effects of variable stiffness, radial loading, axial forces, and thermal deformation [4]. In recent years, nonlinear bending and thermoelastic analysis of plates and shells have attracted increasing attention due to their importance in lightweight, aerospace, mechanical, marine, and energy structures. Recent works have considered nonlinear bending of nanocomposite cylindrical shells under mechanical loading, nonlinear static bending of microplates on elastic foundations, variable-thickness functionally graded plates, rotating thermoelastic cylindrical shells, and cylindrical shells under complex combined loading. These studies show that variable geometry, non-uniform material or thermal fields [5], and nonlinear deformation effects significantly influence the stiffness, deflection, buckling, and stress response of thin-walled structures. Nevertheless, many existing approaches rely mainly on finite element, isogeometric, or fully numerical procedures. Although such methods are powerful, analytical-discrete formulations remain useful because they provide explicit relationships between load, thickness variation, thermal parameters, boundary conditions, and shell response [6]. Therefore, the present work contributes to this field by developing an analytical-discrete solution for a closed cylindrical shell of variable thickness subjected to axisymmetric mechanical loading and a non-uniform temperature field.

## 2. Materials and methods

### 2.1. Problem statements

To improve the transparency of the analytical procedure, the solution is obtained in the following sequence. First, the shell thickness is prescribed by the linear law $h(z) = h_0 + kh_1 z$, which defines the variable bending stiffness $D(z) = \frac{Eh^3}{12(1-\mu^2)}$. Second, the non-uniform temperature field is represented by the functions $f(z) = \beta_0 + \beta_1 z + \beta_2 z^2$ and $F(z) = \alpha_0 + \alpha_1 z$. These expressions are substituted into the governing equilibrium equation, after which the temperature-dependent terms are explicitly simplified. Third, the membrane contribution containing $u(z)$ is represented using partial discretization over the axial coordinate. This transformation preserves analytical integration of the remaining differential equation while introducing nodal displacement contributions [1]. Fourth, the resulting equation is integrated successively to obtain expressions for the radial deflection $u(z)$, rotation angle $du/dz$, meridional bending moment $M_1(z)$, and transverse shear force $Q(z)$. Finally, the integration constants are determined by imposing the boundary conditions of a rigidly clamped lower edge and a free upper edge. This step-by-step formulation provides a reproducible analytical procedure for evaluating the bending response of a variable-thickness cylindrical shell under combined mechanical and thermal loading. The plate is subjected to an axisymmetric shear load distributed along the circle $r = r_C$. In the generalized function representation, the load function is written as $\Psi = \frac{1}{r}\int_0^r q_0 \delta(r - r_c) r dr$, where $q_0$ is the load intensity and $\delta(r - r_c)$ is the Dirac delta function. All field variables depend only on the radial coordinate $r$.

### 2.2. Mathematical model

The nonlinear governing equations of the rotationally symmetric plate in terms of the deflection $w(r)$ and the stress function $\Phi(r)$ are:

$$D\frac{d}{dr}(\nabla^2 w) = \Psi + \frac{h}{r}\frac{d\Phi}{dr}\frac{dw}{dr}, \quad \frac{d}{dr}(\nabla^2 \Phi) = -\frac{E}{2r}\left(\frac{dw}{dr}\right)^2, \quad \nabla^2 = \frac{1}{r}\frac{d}{dr}\left(r\frac{d}{dr}\right). \tag{1}$$

Applying Tyurekhodzhaev's partial discretization to the second Eq. (1), the nonlinear term is localized at the nodal radii $r_k$, $k = 1,2,\dots,n$, and the equation takes the form:

$$\begin{aligned}\frac{d^3\Phi}{dr^3} + \frac{1}{r}\frac{d^2\Phi}{dr^2} - \frac{1}{r^2}\frac{d\Phi}{dr} \\ = -\frac{E}{4r}\sum_{k=1}^{n}(r_k + r_{k+1})\left\{\left[\frac{dw(r_k)}{dr}\right]^2 \delta(r - r_k) - \left[\frac{dw(r_{k+1})}{dr}\right]^2 \delta(r - r_{k+1})\right\}.\end{aligned} \tag{2}$$

The general solution of Eq. (2) for the stress-function derivative is:

$$\begin{aligned}\frac{d\Phi}{dr} &= C_1 r + C_2\frac{1}{r} - \frac{E}{8}\sum_{k=1}^{n}\left\{\left[\frac{dw(r_k)}{dr}\right]^2\left(1+\frac{r_{k+1}}{r_k}\right)\left(r-\frac{{r_k}^2}{r}\right)H(r-r_k)\right.\\ &\left.-\left[\frac{dw(r_{k+1})}{dr}\right]^2\left(1+\frac{r_k}{r_{k+1}}\right)\left(r-\frac{{r_{k+1}}^2}{r}\right)H(r-r_{k+1})\right\},\end{aligned} \tag{3}$$

where $H$ is the Heaviside step function and $C_1$, $C_2$ are integration constants. Substituting Eq. (3) into the first Eq. (1) and partially discretizing the factor $dw/dr$ yields an integro-discrete equation for the slope:

$$\begin{aligned}&\frac{d^3w}{dr^3}+\frac{1}{r}\frac{d^2w}{dr^2}-\frac{1}{r^2}\frac{dw}{dr}\\ &=\frac{1}{D}\left[\Psi+\frac{h}{r}\left(C_1 r + C_2\frac{1}{r} - \frac{E}{8}\sum_{k=1}^{n}\left\{\left[\frac{dw(r_k)}{dr}\right]^2\left(1+\frac{r_{k+1}}{r_k}\right)\left(r-\frac{{r_k}^2}{r}\right)H(r-r_k)\right.\right.\right.\\ &-\left[\frac{dw(r_{k+1})}{dr}\right]^2\left(1+\frac{r_k}{r_{k+1}}\right)\left(r-\frac{{r_{k+1}}^2}{r}\right)H(r-r_{k+1})\right\}\sum_{k+1}^{n}\frac{1}{2}(r_k+r_{k+1})\left\{\left[\frac{dw(r_k)}{dr}\right]\delta(r\right.\\ &\left.\left.\left.-r_k)-\left[\frac{dw(r_{k+1})}{dr}\right]\delta(r-r_{k+1})\right\}\right)\right],\end{aligned} \tag{4}$$

where the subscript $pd$ indicates the partially discretized nonlinear product. Integration of Eq. (4), with due account of the properties of discontinuous generalized functions [2], gives Eq. (5) the slope in the form:

$$\begin{aligned}\frac{dw}{dr} &= C_3\frac{r}{2}+C_4\frac{1}{r}\\ &+\frac{1}{D}\left[\frac{1}{r}\int\left(r\int\Psi(r)\,dr\right)dr\right.\\ &+\frac{hr}{4}\left\{(r_1+r_2)\left(C_1+C_2\frac{1}{{r_1}^2}\right)\left(1-\frac{{r_1}^2}{r^2}\right)\left[\frac{dw(r_1)}{dr}\right]H(r-r_1)+\right.\\ &\left.+\sum_{i=2}^{n}(r_{i+1}-r_{i-1})\left(C_1+C_2\frac{1}{{r_i}^2}\right)\left(1-\frac{{r_i}^2}{r^2}\right)\left[\frac{dw(r_i)}{dr}\right]H(r-r_i)\right\}\\ &-\frac{Ehr}{32}\left(1+\frac{r_2}{r_1}\right)\sum_{k=2}^{n}(r_{k+1}-r_{k-1})\left\{\left(1-\frac{{r_1}^2}{{r_k}^2}\right)\times\left(1-\frac{{r_k}^2}{r^2}\right)\left[\frac{dw(r_1)}{dr}\right]^2\right.\\ &\left.\left.+\sum_{j=2}^{k-1}\frac{(r_{j+1}-r_{j-1})}{r_j}\left(1-\frac{{r_j}^2}{{r_k}^2}\right)\left(1-\frac{{r_k}^2}{r^2}\right)\left[\frac{dw(r_k)}{dr}\right]^2\right\}\left[\frac{dw(r_k)}{dr}\right]H(r-r_k)\right].\end{aligned} \tag{5}$$

Regularity of $d\Phi/\mathrm{dr}$ and $dw/dr$ at $r=0$, $C_2=C_4=0$. Consequently, the reduced expressions Eq. (6) and Eq. (7) for the stress-function derivative and slope become:

$$\begin{aligned}\frac{d\Phi}{dr} &= C_1 r - \frac{Er}{8}\left\{\left(1+\frac{r_2}{r_1}\right)\left(1-\frac{r_1^2}{r^2}\right)\left[\frac{dw(r_1)}{dr}\right]^2 H(r-r_1)\right.\\ &\left.+\sum_{k=2}^{n}\frac{(r_{k+1}-r_{k-1})}{r_k}\left(1-\frac{{r_k}^2}{r^2}\right)\left[\frac{dw(r_k)}{dr}\right]^2 H(r-r_k)\right\},\end{aligned} \tag{6}$$

$$\frac{dw}{dr} = C_3\frac{r}{2} + \frac{q_0({r_b}^2 - {r_a}^2)^2}{4Dr}\left(\ln\frac{r_b}{r_a} - \frac{1}{2}\right) + \Phi_{ln}(r), \tag{7}$$

where $\Phi_{nl}(r)$ denotes the complete nonlinear nodal contribution obtained from the partial discretization procedure.

The boundary conditions for the annular plate are prescribed as:

$$\begin{gathered}\sigma_r(r) = \frac{1}{r}\frac{d\Phi}{dr} = \sigma_0, \quad r = r_a, \quad M_r(r) = -D\left(\frac{d^2w}{d^2r} + \frac{\mu}{r}\frac{dw}{dr}\right) = 0, \\ r = r_b, \quad w(r) = 0, \quad r = r_C.\end{gathered} \tag{8}$$

Application of boundary conditions Eq. (8) provides the final closed-form expressions for the deflection, stress components, and bending moments [3]. To preserve the complete mathematical model in compact conference form, the resulting relations are summarized below:

$$w(r) = w_q(r, q_0, r_a, r_b, r_C, \mu) + w_\sigma(r, \sigma_0, r_k, \mu) + w_{nl}(r, E, h, r_k), \tag{9}$$

$$\begin{aligned}\sigma_r(r) = \sigma_0 - \frac{E}{8}\Bigg\{&\left(1 + \frac{r_2}{r_1}\right)\left(1 - \frac{r_1^2}{r^2}\right)\left[\frac{dw(r_1)}{dr}\right]^2 H(r - r_1) \\ &+ \sum_{k=2}^{n}\frac{(r_{k+1} - r_{k-1})}{r_k}\left(1 - \frac{r_k^2}{r^2}\right)\left[\frac{dw(r_k)}{dr}\right]^2 H(r - r_k)\Bigg\},\end{aligned} \tag{10}$$

$$\begin{aligned}\sigma_\theta(r) = \sigma_0 - \frac{E}{8}\Bigg\{&\left(1 + \frac{r_2}{r_1}\right)\left(1 + \frac{r_1^2}{r^2}\right)\left[\frac{dw(r_1)}{dr}\right]^2 H(r - r_1) \\ &+ \sum_{k=2}^{n}\frac{(r_{k+1} - r_{k-1})}{r_k}\left(1 + \frac{r_k^2}{r^2}\right)\left[\frac{dw(r_k)}{dr}\right]^2 H(r - r_k)\Bigg\},\end{aligned} \tag{11}$$

$$M_r(r) = M_r^{q(r)} + M_r^{\sigma(r)} + M_r^{nl(r)}, \quad M_\theta(r) = M_\theta^{q(r)} + M_\theta^{\sigma(r)} + M_\theta^{nl(r)}, \tag{12}$$

where, the superscripts $q$, $\sigma$ and $nl$ denote, respectively, the contributions of the transverse load, radial boundary stress, and nonlinear nodal interaction terms. Eq. (9) to Eq. (12) constitute the complete analytical model and are the basis for the engineering interpretation presented in the next section.

### 2.3. Explicit stress-resultant relations

The compact notation used in Eq. (9) to Eq. (12) may be expanded to emphasize the structure of the final analytical solution [4]. The deflection is represented as the sum of a load-controlled contribution, a membrane-stress contribution, and a nonlinear nodal-interaction term. In symbolic form:

$$\begin{aligned}&w(r) = w_q(r) + w_\sigma(r) + w_{nl}(r), \\ &w_q(r) = -\frac{q_0 r_c r^2}{4D}\Bigg\{A_1\left[\left(1 - \frac{{r_c}^2}{r^2}\right) - \frac{{r_b}^2}{r^2}\left(1 - \frac{{r_c}^2}{{r_b}^2}\right)\right] \\ &\quad + \left[\left(1 - \frac{{r_c}^2}{r^2}\right) - \ln\frac{r}{r_c}\left(1 + \frac{{r_c}^2}{r^2}\right)\right]H(r - r_c) - A_2\Bigg\}, \\ &A_1 = \ln\frac{r_b}{r_c} + \left[\frac{(1-\mu)}{2(1+\mu)}\right]\left(1 - \frac{{r_c}^2}{{r_b}^2}\right), \quad A_2 = \left(1 - \frac{{r_c}^2}{{r_b}^2}\right) - ln\frac{r_b}{r_c}\left(1 + \frac{{r_c}^2}{{r_b}^2}\right).\end{aligned} \tag{13}$$

The stress-controlled part $w_\sigma(r)$ and the nonlinear term $w_{nl}(r)$ Eq. (13) are written through the nodal quantities $dw(r)/dr$, the radius ratios $r_i/r$ and $r_i/r_b$, and the Heaviside functions $H(r-r_i)$. In this form the complete deflection relation remains explicit while preserving the full nonlinear interaction generated by partial discretization [5].

The final stress components Eq. (14) to Eq. (16) derived from the stress function and the deflection slope are:

$$\sigma_r(r) = \frac{\left(\frac{1}{r}\right) d\Phi}{dr}, \quad \sigma_\theta(r) = \frac{d^2\Phi}{dr^2}, \tag{14}$$

$$\sigma_r(r) = \sigma_0 - \frac{E}{8}\left\{B_1(r)\left[\frac{dw(r_1)}{dr}\right]^2 H(r-r_1) + \sum_{k=2}^{n} B_k(r)\left[\frac{dw(r_k)}{dr}\right]^2 H(r-r_k)\right\}, \tag{15}$$

$$\sigma_\theta(r) = \sigma_0 - \frac{E}{8}\left\{C_1(r)\left[\frac{dw(r_1)}{dr}\right]^2 H(r-r_1) + \sum_{k=2}^{n} C_k(r)\left[\frac{dw(r_k)}{dr}\right]^2 H(r-r_k)\right\}, \tag{16}$$

$$\begin{aligned} B_1(r) &= \left(1+\frac{r_2}{r_1}\right)\left(1-\frac{{r_1}^2}{r^2}\right), \quad C_1(r) = \left(1+\frac{r_2}{r_1}\right)\left(1+\frac{{r_1}^2}{r^2}\right), \\ B_k(r) &= \left[\frac{(r_{k+1}-r_{k-1})}{r_k}\right]\left(1-\frac{{r_k}^2}{r^2}\right), \quad C_k(r) = \left[\frac{(r_{k+1}-r_{k-1})}{r_k}\right]\left(1+\frac{{r_k}^2}{r^2}\right). \end{aligned} \tag{17}$$

Similarly, the radial and circumferential bending moments can be written directly in terms of curvature and slope:

$$M_r(r) = -D\left[\frac{d^2w}{dr^2} + \frac{\left(\frac{\mu}{r}\right) dw}{dr}\right], \quad M_\theta(r) = -D\left[\mu\frac{d^2w}{dr^2} + \frac{1}{r\frac{dw}{dr}} + \right]. \tag{18}$$

After substituting the explicit partially discretized slope and deflection expressions into Eq. (18), both moment resultants split naturally into load, stress [6], and nonlinear parts, as indicated in Eq. (12). This decomposition is convenient in engineering interpretation because it identifies the relative contribution of each physical mechanism.

For comparative studies it is also useful to introduce the nondimensional radius and deflection:

$$\rho = \frac{r}{r_b}, \quad \varkappa = \frac{wD}{q_0 {r_b}^4}, \tag{19}$$

which allow plates of different stiffness and geometry Eq. (19) to be compared on a common basis.

## 3. Results and discussion

To provide additional quantitative evidence of the effect of radial boundary load on the deformation behavior of the shell, a statistical analysis was carried out for several values of the radial load $P$. For each loading case, the radial deflection $u(z)$ was evaluated along the shell length, and the main statistical characteristics were calculated. These included the mean deflection $u(P_i)$, maximum deflection $u_{max}(P_i)$, standard deviation $\sigma_u(P_i)$, coefficient of variation $CV_{P_i} = \frac{\sigma_u(P_i)}{u(P_i)} \times 100$ %, and relative increase in deflection compared with the reference load case. The statistical results confirm that the increase in radial load leads to a monotonic increase in both the mean and maximum values of radial deflection. For example, when the load is increased from $P_i \in \{2\times10^3,\ 4\times10^3,\ 6\times10^3\}$ N/m$^2$, the calculated deflection curves show a corresponding systematic increase in deformation magnitude. This confirms that the radial load is one of the dominant factors controlling the bending response of the cylindrical shell. In addition to deterministic curves, probability-based plots were constructed to characterize the distribution of deflection values along the shell length. The histogram and probability density function show how the calculated deflection values are distributed for each loading case, while the cumulative distribution function describes the probability that the radial deflection does not exceed a specified value. The reliability-type curve $R(u) = P(U > u)$ was also used to estimate the probability of exceeding a selected deformation threshold. A regression-based scatter plot of radial load versus maximum deflection further confirms the strong dependence between $P$ and $u_{max}$. The trend line demonstrates that the maximum deflection increases nearly proportionally with the radial load within the considered loading interval. Therefore, the statistical and probabilistic analysis supports the analytical solution and provides additional evidence that radial boundary loading has a significant effect on the deformation behavior of the shell.

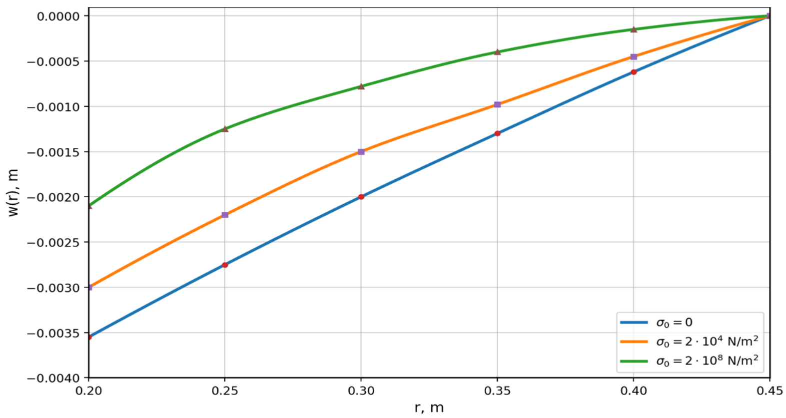


**Fig. 1.** Deflection curves of the annular plate for different values of the radial stress $\sigma_0$ applied at the inner boundary: $\sigma_0 = 0$, $\sigma_0 = 2\times10^4$ N/m$^2$, and $\sigma_0 = 2\times10^8$ N/m$^2$. The calculations were performed for $h = 0.02$ m, $q_0 = 2.5\times10^5$ N/m$^2$, $E = 2\times10^{11}$ N/m$^2$, $\mu = 0.3$

Fig. 1 illustrates the statistical and probabilistic evaluation was performed using the calculated deflection values $u(z_j, p_i)$, where $P_i \in \{2\times10^3, 4\times10^3, 6\times10^3\}$ N/m$^2$. For each load case, the mean value, maximum value, standard deviation, coefficient of variation, relative increase, and exceedance probability were determined.

## 4. Conclusions

In this study, an analytical solution for the flexure problem of a rotationally symmetric circular plate was developed using the method of partial discretization of differential equations. The proposed approach makes it possible to transform the governing fourth-order differential equation into an analytical-discrete form that is convenient for evaluating the deformation and internal force characteristics of the plate. These expressions allow the influence of radial boundary load and transverse loading on the deformation behavior of the plate to be analyzed in a direct and physically interpretable form. The obtained results demonstrate that an increase in radial boundary load leads to a systematic increase in the plate deflection and affects the distribution of internal force factors. The graphical results confirm the effectiveness of the proposed analytical formulation. Comparative curves for different loading cases show that the radial boundary load is one of the key parameters controlling the flexural response of the plate. In addition, the introduced statistical and probabilistic evaluation provides quantitative confirmation of this effect through the mean deflection, maximum deflection, standard deviation, coefficient of variation, and exceedance probability. The proposed method is useful for fundamental studies of plate bending because it preserves the analytical structure of the solution while allowing complex loading effects to be included through partial discretization. The obtained formulation may be applied to circular plates and thin structural elements used in mechanical, civil, aerospace, and energy engineering.

## Acknowledgements

The authors have not disclosed any funding.

## Data availability

The datasets generated during and/or analyzed during the current study are available from the corresponding author on reasonable request.

## Conflict of interest

The authors declare that they have no conflict of interest.

## References

**[1]** D.-G. Zhang, "Analytical solutions for nonlinear axisymmetric deformations of circular plates by using innovative orthogonal power function series," *Archive of Applied Mechanics*, Vol. 94, No. 10, pp. 2877–2887, Jul. 2024, https://doi.org/10.1007/s00419-024-02648-9

**[2]** X.-T. He, B. Pang, J.-C. Ai, and J.-Y. Sun, "Functionally graded thin circular plates with different moduli in tension and compression: improved Föppl-von Kármán equations and its biparametric perturbation solution," *Mathematics*, Vol. 10, No. 19, p. 3459, Sep. 2022, https://doi.org/10.3390/math10193459

**[3]** J. Kim, E. Nava, and S. Rakici, "Nonlinear finite element model for bending analysis of functionally-graded porous circular/annular micro-plates under thermomechanical loads using quasi-3D Reddy third-order plate theory," *Materials*, Vol. 16, No. 9, p. 3505, May 2023, https://doi.org/10.3390/ma16093505

**[4]** S. G. M. Doori, A. R. Noori, and A. Etemadi, "Static response of functionally graded porous circular plates via finite element method," *Arabian Journal for Science and Engineering*, Vol. 49, No. 10, pp. 14167–14181, Mar. 2024, https://doi.org/10.1007/s13369-024-08914-w

**[5]** K. Benazouz, H. Bechir, and A. Djema, "Modeling nonlinear bending of axisymmetric circular nano-plates in framework of Ru's surface stress elasticity theory," *Journal of Engineering Mathematics*, Vol. 132, No. 1, p. 6, Dec. 2021, https://doi.org/10.1007/s10665-021-10192-6

**[6]** E. Rahimi, M. Sadeghian, and M. E. Golmakani, "Nonlinear bending examination of nanocomposite cylindrical shell exposed to mechanical loads using dynamic relaxation method," *Proceedings of the Institution of Mechanical Engineers, Part N: Journal of Nanomaterials, Nanoengineering and Nanosystems*, Vol. 239, No. 3-4, pp. 273–289, Feb. 2024, https://doi.org/10.1177/23977914231215229